

Cite this: *Chem. Sci.*, 2022, **13**, 9351

All publication charges for this article have been paid for by the Royal Society of Chemistry

Received 5th April 2022
Accepted 8th July 2022

DOI: 10.1039/d2sc01966c
rsc.li/chemical-science

Introduction

Gold catalysis has been dominated by the Lewis acidity of gold towards activation of alkenes and alkynes for nucleophilic attacks.^{1–6} On the other hand, redox Au(i)/Au(III) catalysis has been less explored and mainly achieved in the presence of sacrificial external oxidants,^{7–17} especially due to the reluctance of Au(i) to undergo oxidative addition.^{18–21} In this regard, several strategies have been explored to overcome this limitation,^{22–46} among which the chelation-assisted strategy in pre-designed ligands^{30–34} or the oxidative addition using strained molecules such as biphenylene stand out.³⁵ Bourissou pioneered in 2014 the intramolecular oxidative addition of C_{sp^2} –X bonds (X = Br, I) at Au(i) by utilizing rigid 8-halonaphthyl phosphine model substrates, which suitably place the C_{sp^2} –X bond close to the Au(i) atom upon coordination

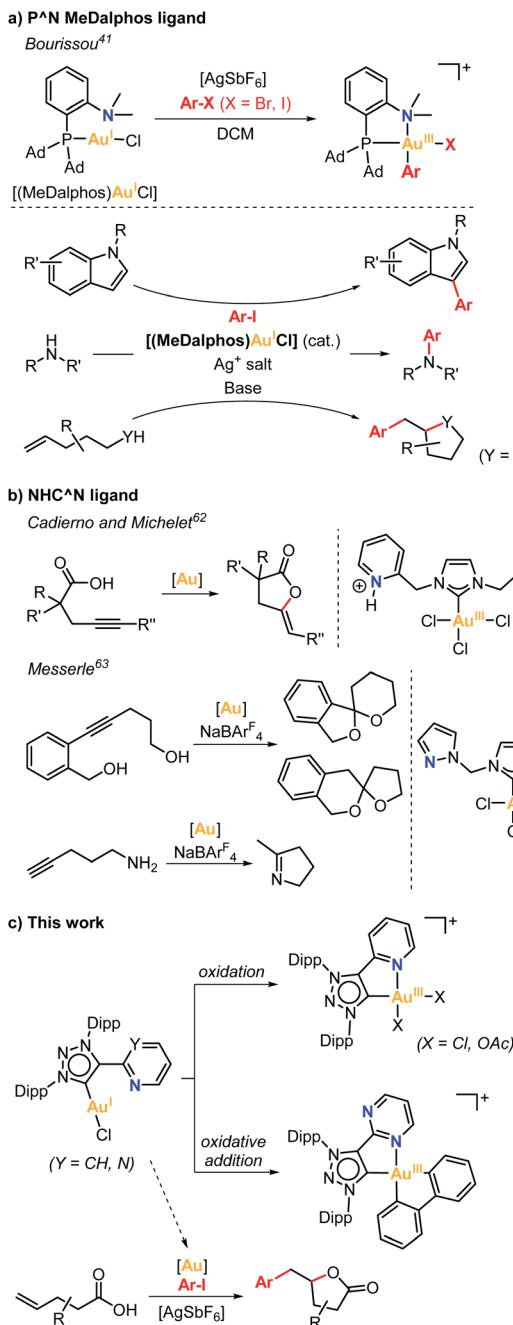
to the phosphine moiety. In this manner, facile stabilization of the (P,C)-cyclometalated Au(III) products is obtained *via* oxidative addition.³² In the same line, Hashmi and Hermange used a similar strategy taking advantage of pendant pyridine groups in monophosphine ligands to stabilize Au(III) systems upon reaction of Au(i) complexes with aryl diazonium salts.^{47,48} In these examples, the subtle change from linear to square-planar geometry is crucial for the facile reactivity of Au(i) species towards a key oxidative addition process. Noteworthy, P^N MeDalphos ligand showed great performance at promoting the oxidative addition of aryl halides at Au(i), as well as at stabilizing Au(III) intermediates, which paved the way to Au(i)/Au(III) catalytic transformations using the (MeDalphos)AuCl catalyst (Scheme 1a).⁴¹ For instance, in 2019 Bourissou and coworkers reported the regioselective Au(i)/Au(III)-catalyzed C3 arylation of indoles, which is rarely attained by other transition metals (Scheme 1a),⁴⁹ additionally they described the Au(i)/Au(III) catalyzed C3 allylation of indoles using allyl alcohols or allyl acetates.⁵⁰ Significantly, two independent reports by the groups of Patil⁵¹ and Bourissou⁵² disclosed the C_{sp^2} –N cross-coupling reactions of aryl iodides with amines mediated by the MeDalphos-enabled Au(i)/Au(III) catalysis (Scheme 1a). In 2020, Bourissou and Patil groups independently showed that the oxidative addition of aryl iodides and π -activation of olefins can be merged by the Au(i)/Au(III) platform using (MeDalphos)AuCl as catalyst, which involves the oxy- and aminoarylation reactions of alkenols and alkenamines (Scheme 1a).^{53,54} The 1,2-heteroarylation of alkenes was also achieved using external alcohols and amines.^{54–56} Interestingly, (MeDalphos)AuCl catalyst has proven to

^a Institut de Química Computacional i Catalisi (IQCC) and Departament de Química, Universitat de Girona, Campus de Montilivi, Girona E-17003, Catalonia, Spain.
E-mail: hugo.valdes@udg.edu; xavi.ribas@udg.edu

^b Departamento de Química Inorgánica, Instituto de Síntesis Química y Catálisis Homogénea (ISQCH), Universidad de Zaragoza-CSIC, Zaragoza 50009, Spain.
E-mail: gguisado@unizar.es

† Electronic supplementary information (ESI) available: For materials, instrumentation, experimental procedures and spectroscopic characterization of all compounds. CCDC 2163608 (**4a**–OAc), 2163609 (**2a**), 2163610 (**2b**), 2163611 (**4a**–Cl), 2163612 (**8a**–OMe), 2163613 (**3b**–biphenylene), 2163614 (**5b**), 2163615 (**6b**), 2163616 (**8b**–OMe), 2163617 (**3a**), 2163877 (**16**) and 2176932 (**cis**–**7a**–Cl) contain the supplementary crystallographic data for this paper. For ESI and crystallographic data in CIF or other electronic format see <https://doi.org/10.1039/d2sc01966c>





Scheme 1 (a) Oxidative addition of aryl halides to a Au(I) complex bearing the hemilabile P^N MeDalphos ligand, and selected examples of its catalytic activity. (b) Selected examples of gold complexes bearing hemilabile NHC^N ligands. (c) Ability of hemilabile MIC^N ligands to stabilize Au(III) complexes obtained from Au(I) via oxidation or via oxidative addition, and application of the (MIC^N)Au(I) complexes to the arylation-lactonization reaction of γ -alkenoic acids.

be a key factor in the development of other transformations such as 1,2-diarylation of alkenes,⁵⁷ or trifluoromethylthiolation and trifluoromethyl-selenolation of organohalides.⁵⁸ Very recently, Shi and Patil groups developed new chiral-hemilabile P^N-ligands to access enantioselective Au(I)/Au(III) catalysis.^{59,60}

In contrast to the well-known P^N ligands, the use of bidentate C^N or C^O ligands⁶¹ remains scarcely explored, and

the few representative examples are depicted in Scheme 1b. Cadierno and Michelet studied the catalytic activity of a (NHC^N)Au(III) complex containing a N-heterocyclic carbene ligand (NHC) with a pyridinium side arm in the cyclization of γ -alkenoic acids (Scheme 1b),⁶² while Messerle and coworkers explored the dihydroalkoxylation and hydroamination catalyzed by a Au(III) complex bearing a NHC ligand with two pendant pyrazole arms (Scheme 1b).⁶³ Alternatively, Bertrand and coworkers showed that a hemilabile bidentate cyclic (alkyl)(amino)carbene (CAAC) Au(I) complex undergoes oxidative addition of biphenylene.⁴⁰

More recently, Bourissou and coworkers reported the reactivity of a Au(I) complex containing a N3-alkylated mesoionic 1,2,3-triazol-5-ylidene bearing a pendant pyridine group.⁶⁴ However, the complex did not undergo oxidative addition towards iodobenzene, thus precluding its exploitation in oxidant-free reactivity. In fact, the formation of a dimeric Au(I) species was observed instead of the formation of the oxidative addition Au(III) product. On the other hand, the Au(I) complex was reactive towards a strong oxidant such as PhICl₂, forming a mononuclear square-planar Au(III) species. The latter experiment demonstrated that mesoionic carbene ligands bearing N-based hemilabile groups (MIC^N) can potentially be suitable platforms to stabilize Au(III) species.

Based on the abovementioned, we herein explore the reactivity of two new (MIC^N)Au(I) complexes bearing hemilabile pyridine (py) or pyrimidine (pym) pendant groups, their ability to stabilize (MIC^N)Au(III) species and their performance in oxidant-free oxidative addition of aryl halides and strained C-C bonds. After proving the successful ability to sustain oxidant-free Au(I)/Au(III) redox processes, we further extended its application to arylation-lactonization reactions of γ -alkenoic acids (Scheme 1c).

Results and discussion

Synthesis and characterization of (MIC^N)Au(I) complexes

Initially, two 1,2,3-triazolium salt precursors (MIC^N) bearing 2,6-diisopropylphenyl substituents (Dipp) at the outer nitrogens of the azolium ring and either a pyridine (**1a**) or a pyrimidine (**1b**) side arm were prepared by following an adapted method reported in the literature (Fig. 1a).⁶⁵ We reacted 1,3-bis(2,6-diisopropylphenyl)triaz-1-ene with 2-ethynylpyridine or 2-ethynylpyrimidine in the presence of *tert*-butyl hypochlorite ('BuOCl) and anhydrous potassium hexafluorophosphate (KPF₆), affording the desired products in high and moderate yield (99% for **1a** and 67% for **1b**). In order to obtain the corresponding (MIC^N)Au(I) complexes, we attempted the Au(I) coordination through a transmetalation reaction to Ag(I) species. For this purpose, we reacted the corresponding triazolium salts with silver oxide (Ag₂O) in the presence of cesium carbonate (Cs₂CO₃) and potassium chloride (KCl) as halide source. Then, the addition of dimethylsulfide gold(I) chloride [AuCl(SMe₂)] immediately produced the precipitation of the silver halide. After purification, the desired Au(I) complexes **2a** and **2b** were obtained in 32% and 35% yield, respectively. The ¹H NMR spectra of the complexes showed the absence of the acidic proton of the triazolium salts, indicating that the

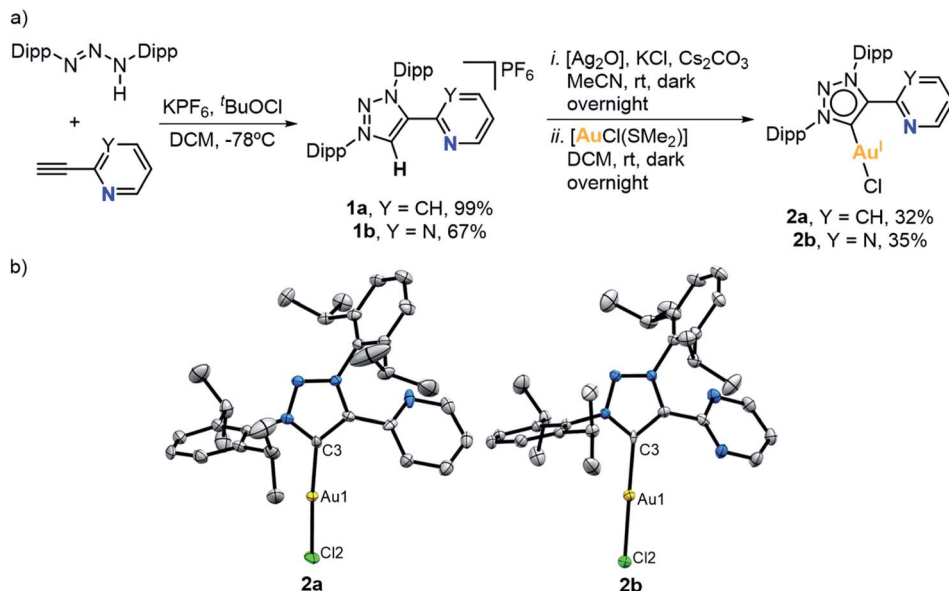


Fig. 1 (a) Synthesis of $\text{Au}^{\text{(I)}}$ complexes **2a** and **2b**. (b) Crystal structures of **2a** and **2b** (ellipsoids set at 50% probability and H atoms removed for clarity). Selected bond distances (\AA): for **2a**, Au1-C3 1.982(6), Au1-Cl2 2.2854(17); for **2b**, Au1-C3 2.006(4), Au1-Cl2 2.2728(16).

coordination to gold had occurred. The $^{13}\text{C}\{\text{H}\}$ NMR spectrum of **2a** showed the characteristic signal of the metallated carbon at 162.1 ppm, while in the case of the pyrimidine derivative **2b**, such signal was slightly shifted downfield, appearing at 165.3 ppm. Furthermore, the molecular structure of both $\text{Au}^{\text{(I)}}$ complexes **2a** and **2b** was unambiguously determined by X-ray diffraction analyses (Fig. 1b). Both complexes are isostructural, showing the mesoionic carbene ligand coordinated to an $\text{Au}^{\text{(I)}}$ atom, and a chlorine ligand completing the linear coordination sphere around the metal (C-Au-Cl angle is 174.31(18) $^{\circ}$ for **2a** and 179.30(9) $^{\circ}$ for **2b**). Noticeably, no coordination of the hemilabile pyridine or pyrimidine moieties at $\text{Au}^{\text{(I)}}$ was observed.

Then, $\text{Au}^{\text{(I)}}$ complexes **2a** and **2b** were reacted with silver hexafluoroantimonate (AgSbF_6) in CD_2Cl_2 at room temperature (Fig. 2a), seeking the engagement of the pendant pyrimidine or pyridine groups in the coordination to $\text{Au}^{\text{(I)}}$. The ^1H NMR spectra of the corresponding complexes showed some changes in the aromatic and aliphatic region. In particular, the signals of the pyridine or pyrimidine fragments were shifted due to gold coordination. The most significant change was observed in the $^{13}\text{C}\{\text{H}\}$ NMR spectra. The signal of the carbenic carbon was shifted from 162.1 to 157.2 ppm in the case of the pyridine derivative (**3a**), and from 165.3 to 161.3 ppm in the case of the pyrimidine derivative (**3b**).

X-ray diffraction analysis of complex **3a** showed a head-to-tail dimeric $\text{Au}^{\text{(I)}}$ species where each ligand is bridging two metals (Fig. 2). The $\text{Au}^{\text{(I)}}$ centers adopted a linear dicoordinate arrangement, showing an aurophilic interaction ($\text{Au}\cdots\text{Au}$ length of 2.8212(4) \AA). Analogously to Bourissou's $(\text{MIC}^{\text{N}})\text{Au}^{\text{(I)}}$ complex,⁶⁴ the formation of a dimeric $\text{Au}^{\text{(I)}}$ species was favored rather than a mononuclear $\text{Au}^{\text{(I)}}$ having both the MIC and py or pym pendant groups coordinated.

Reactivity of $(\text{MIC}^{\text{N}})\text{Au}^{\text{(I)}}$ complexes with external oxidants and towards oxidative addition

In order to promote the coordination of the side arms of our MIC^{N} ligands, we attempted the 2e^- chemical oxidation of the $\text{Au}^{\text{(I)}}$ complexes to mononuclear $\text{Au}^{\text{(III)}}$. To that end, we studied the reactivity of complex **2a** against a 2e^- oxidant, namely PhIX_2 ($\text{X} = \text{Cl}$ or OAc) (Fig. 2a). The reaction was performed at low temperature, from $-80\text{ }^{\circ}\text{C}$ to rt , in the presence of AgSbF_6 as halogen scavenger. Gratifyingly, the oxidation of $\text{Au}^{\text{(I)}}$ to $\text{Au}^{\text{(III)}}$ took place, with the concomitant coordination of the pendant N -moiety to gold. The $^{13}\text{C}\{\text{H}\}$ NMR spectra of the resulting complexes **4a-Cl** and **4a-OAc** showed the characteristic signal of the carbenic carbon at higher field when compared to the $\text{Au}^{\text{(I)}}$ analogue **2a** (147.3 ppm for **4a-Cl** and 137.1 ppm for **4a-OAc** vs. 162.1 ppm for **2a**). The molecular structures of complexes **4a-Cl** and **4a-OAc** were elucidated by X-ray diffraction analyses (Fig. 2b). Both complexes showed a similar arrangement, *i.e.* the bidentate MIC^{N} ligand coordinated to $\text{Au}^{\text{(III)}}$, and two chlorides or acetates completing its tetracoordinated $\text{Au}^{\text{(III)}}$ center, which featured a slightly distorted square planar geometry. The $\text{C}_{\text{carbene}}\text{-Au}^{\text{(III)}}$ lengths were slightly longer than those found in the $\text{Au}^{\text{(I)}}$ analogue (2.017(8) \AA for **4a-Cl** and 1.991(11) \AA for **4a-OAc** vs. 1.982(6) \AA for **2a**).

At this point, we had demonstrated that these MIC^{N} ligands are indeed suitable platforms to stabilize $\text{Au}^{\text{(III)}}$ species. Thus, we were encouraged to explore the possibility of obtaining $\text{Au}^{\text{(III)}}$ complexes *via* oxidative addition. With this aim, we first attempted the oxidative addition of complex **2b** towards the strained $\text{C}_{\text{sp}}^2\text{-C}_{\text{sp}}^2$ bond of biphenylene, by mixing equimolar amount of **2b** and biphenylene in dichloromethane, in the presence of a halide scavenger, from $-80\text{ }^{\circ}\text{C}$ to room temperature for 10 minutes (Fig. 3a). Unfortunately, we did not observe the desired $\text{Au}^{\text{(III)}}$ center with a biphenyl moiety but,

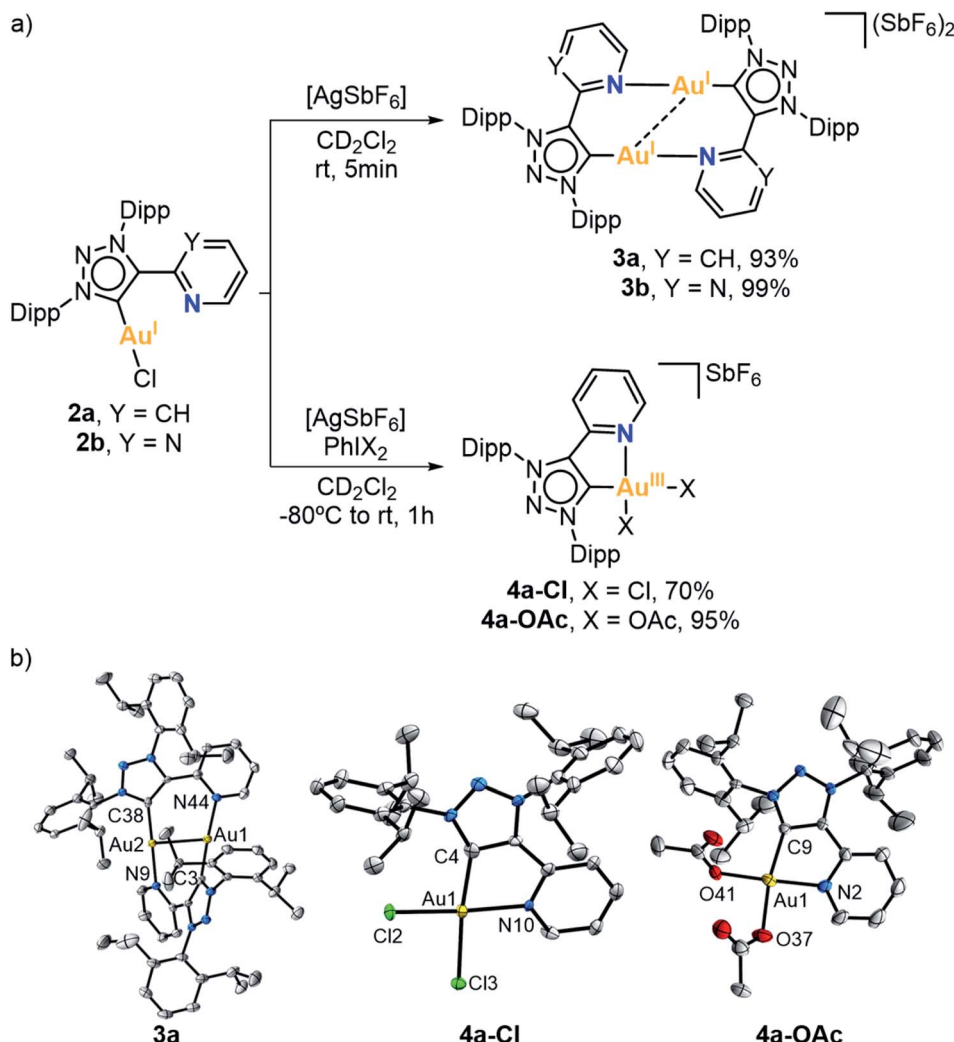


Fig. 2 (a) Reactivity of Au(I) complexes **2a** and **2b** towards halogen scavengers and strong oxidants. (b) Crystal structures of **3a**, **4a-Cl** and **4a-OAc** (ellipsoids set at 50% probability, H atoms and SbF_6^- anions removed for clarity). Selected bond distances (\AA): for **3a**, Au1-Au2 2.8212(4), Au1-N44 2.078(6), Au1-C3 1.988(8), Au2-N9 2.069(6), Au2-C38 1.990(8); for **4a-Cl**, Au1-C4 2.017(8), Au1-N10 2.089(6), Au1-Cl2 2.268(2), Au1-Cl3 2.302(2); for **4a-OAc**, Au1-C9 1.991(11), Au1-N2 2.052(11), Au1-O37 2.032(10), Au1-O41 1.998(9).

interestingly, crystallization of the reaction mixture revealed the co-crystallization of the dimeric complex **3b** with intact biphenylene (**3b**·biphenylene) (Fig. 3b). Even after 5 hours at 50 °C, the outcome of the reaction remained the same. To our delight, when the reaction was heated at 90 °C for 2 hours in 1,2-dichloroethane, the Au(I) center underwent oxidative addition of the strained biphenylene $\text{C}_{\text{sp}}^2-\text{C}_{\text{sp}}^2$ bond, forming the expected Au(III) complex **5b** (Fig. 3a). Notably, the presence of a chloride source (such as KCl or tetrabutylammonium chloride) displaced the hemilabile pyrimidine, affording a neutral Au(III) species, **6b**. By adding AgSbF_6 as halide scavenger, we could reversibly form complex **5b**, also reinforcing the hemilabile character of the pyrimidine moiety. Indeed, the NMR spectra of **5b** showed a dynamic behaviour of the pyrimidine pendant arm, even at 248 K, as indicated by ^1H , ^1H -NOESY experiment (Fig. S49†). Both the cationic **5b** and the neutral **6b** Au(III) species were characterized by X-ray diffraction analyses (Fig. 3b), confirming the weak coordination of the

pyrimidine moiety with a long $\text{Au(III)-N}_{\text{pyrimidine}}$ bond of 2.254 Å for **5b**. The carbene resonance signals were downfield shifted to 182.8 and 180.1 ppm for **5b** and **6b**, respectively.

We then explored the possibility of Au(I) complexes **2a** and **2b** to undergo oxidative addition of $\text{C}_{\text{sp}}^2-\text{I}$ bonds (Fig. 4a). For this purpose, we reacted the Au(I) complexes with *para*-substituted iodoaryls ($\text{R} = \text{OMe, Me, F}$) in the presence of AgSbF_6 , in 1,2-dichloroethane and heating at 120 °C overnight. Unexpectedly, no Au-containing compounds were isolated, but on the contrary, the ^1H NMR and mass spectra were consistent with the full conversion to three triazolium salts (**8a-R**, **9a**, and **1a** when **2a** was used, and **8b-R**, **9b** and **1b** when **2b** was used; $\text{R} = \text{OMe, Me, F}$) (see yields in Fig. 4a). When using **2a** with 4-iodoanisole, the triazolium salts **8a-OMe** and **9a** were unambiguously characterized by X-ray diffraction. Both species co-crystallized, and the single crystal X-ray analysis revealed the presence of **8a-OMe** and **9a** in a 0.89 : 0.11 ratio (Fig. 4b). Likewise, when **2b** was reacted with 4-iodoanisole, the major product was **8b-OMe** with

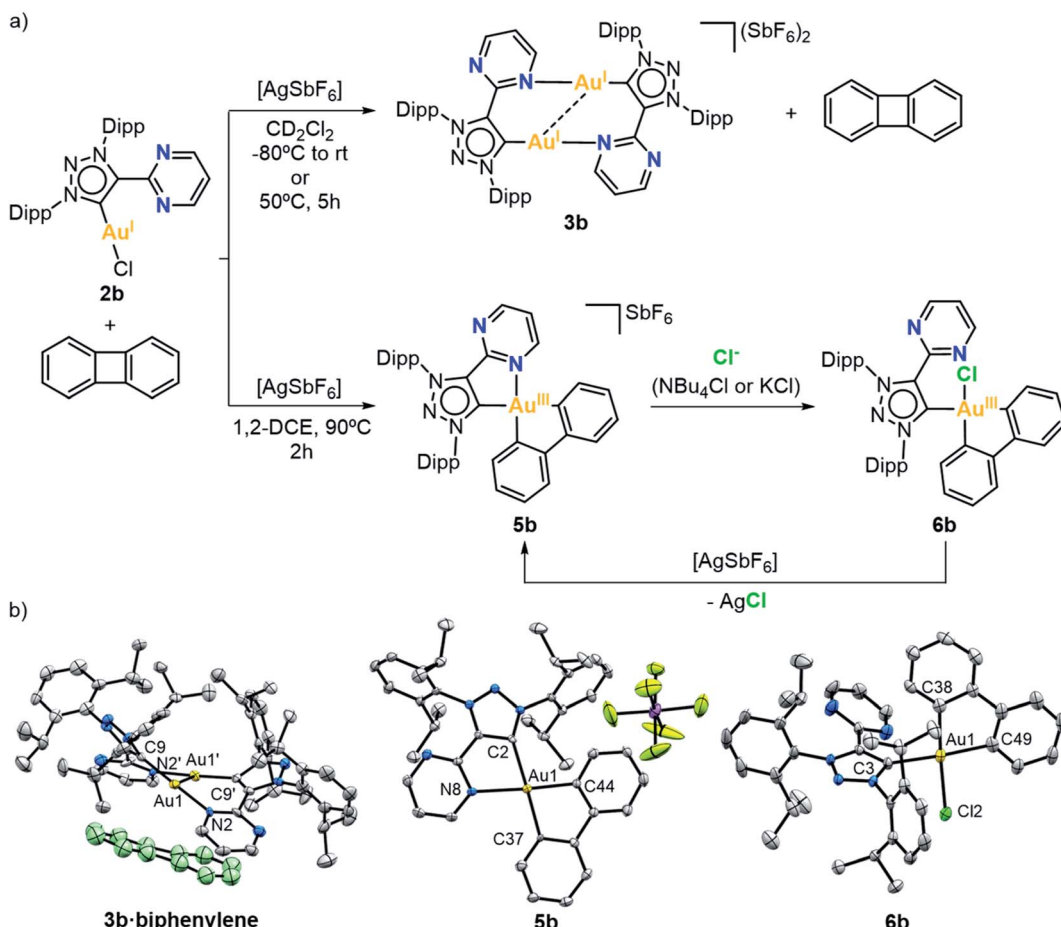


Fig. 3 (a) Study of the reaction conditions for the oxidative addition of a strained $\text{C}_{\text{sp}^2}-\text{C}_{\text{sp}^2}$ bond to complex 2b. (b) Crystal structures of 3b-biphenylene, 5b and 6b (ellipsoids set at 50% probability, H atoms removed for clarity; in the case of 3b-biphenylene the SbF_6^- anions have been removed and the biphenylene molecule is painted in green for clarity). Selected bond distances (Å): for 3b-biphenylene, $\text{Au1}-\text{Au1}'$ 2.8768(10), $\text{Au1}-\text{N2}$ 2.105(8), $\text{Au1}-\text{C9}$ 2.027(10); for 5b, $\text{Au1}-\text{C2}$ 2.108(5), $\text{Au1}-\text{N8}$ 2.254(5), $\text{Au1}-\text{C37}$ 2.066(5), $\text{Au1}-\text{C44}$ 2.019(5); for 6b, $\text{Au1}-\text{C3}$ 2.080(6), $\text{Au1}-\text{Cl2}$ 2.376(3), $\text{Au1}-\text{C38}$ 2.072(7), $\text{Au1}-\text{C49}$ 2.057(7).

a 65% NMR yield, whereas **9b** and **1b** were both obtained in 16% NMR yield. In this case, **8b-OMe** could be isolated and characterized by ^1H NMR, HRMS and X-ray diffraction (Fig. 4b). The formation of such compounds suggested that gold(i) compounds underwent oxidative addition of the aryl iodide followed by a fast reductive elimination of the mesoionic carbene ligand either with the aryl or the iodide moiety coordinated in *cis*, respectively (Fig. 4a). Interestingly, products **8a-R/8b-R** were obtained in higher yields than **9a/9b**, indicating that after the oxidative addition the major product is the one with the aryl ligand in *cis* (**cis-7a-I** or **cis-7b-I**), probably due to the *trans* effect of the NHC ligand. By an alternative route,⁴⁷ the analogous complex **cis-7a-Cl** was synthesized through the oxidative addition of an aryl diazonium salt promoted by blue LED irradiation ($\lambda = 447$ nm). This methodology has the advantage to occur at 25°C , allowing the isolation and fully characterization of the Au(III) species **cis-7a-Cl** (see XRD in Fig. 4b). When **cis-7a-Cl** was heated at 120°C overnight in 1,2-DCE, product **8a-OMe** was formed in 96% yield. This reaction supports that the formation of **8a-R/8b-R** and **9a/9b** from Au(i)

complexes **2a/2b** proceeds *via* an oxidative addition/reductive elimination pathway. We hypothesize that the hemilabile character of the nitrogen atom and the fast decomposition of Au(III) at high temperatures promote the reductive elimination process, which has only been observed, to our knowledge, for a 1,2,3-triazol-5-ylidene based palladium complex.⁶⁶⁻⁶⁸ Nevertheless, our observations sharply contrasted with the lack of reactivity described by Bourissou for a similar $(\text{MIC}^{\text{N}})\text{Au}(\text{i})$ system with aryl iodides.⁶⁴

Arylation-lactonization of γ -alkenoic acids

Based on the successful catalytic application of the P^{N} hemilabile ligand strategy, we envisioned that our hemilabile $(\text{MIC}^{\text{N}})\text{Au}(\text{i})$ complexes may also mediate a cascade reaction involving the key oxidative addition step. Recently, Bourissou and coworkers described the coupling/cyclization reaction of aryl iodides with alkenol and alkenamine compounds catalyzed by a hemilabile P^{N} MeDalPhos/Au(i) system.⁵³ Additionally, in 2017, Shi and coworkers reported a system that afforded coupling/cyclization products upon reacting aryl diazonium

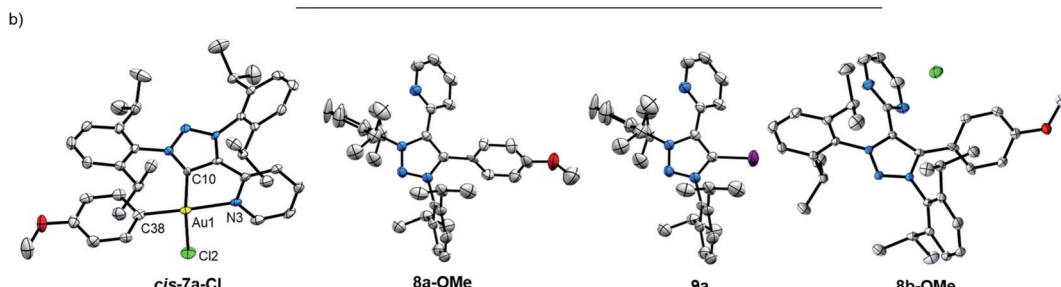
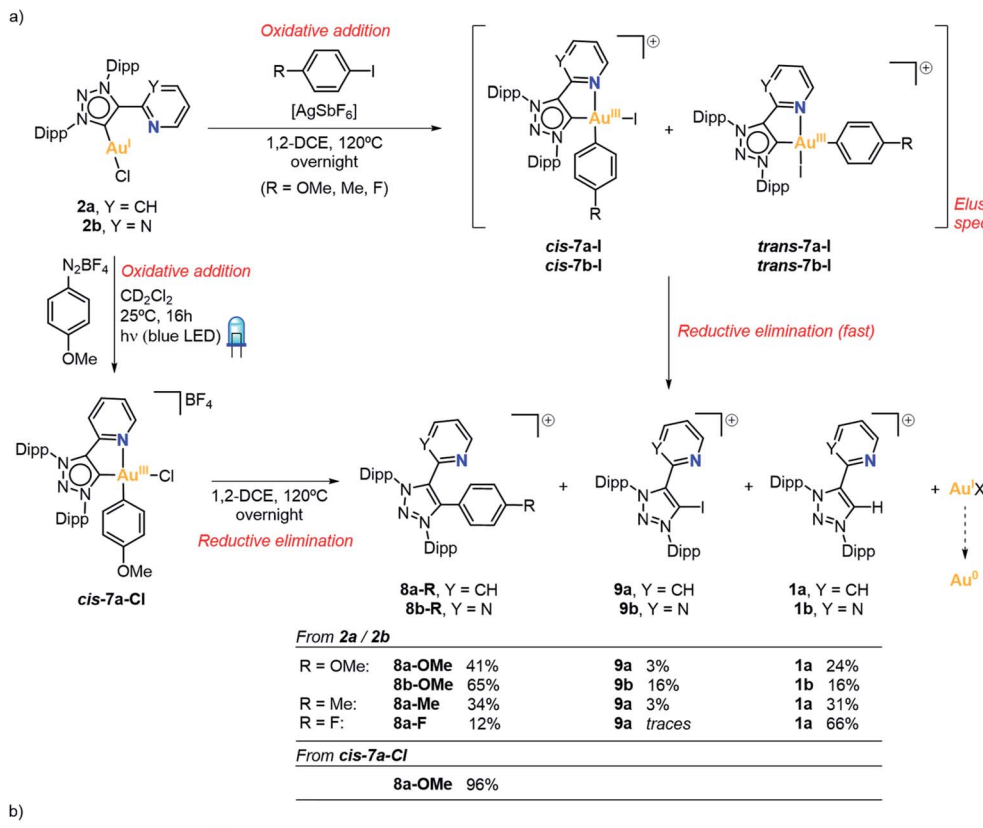


Fig. 4 (a) Reactivity towards aryl iodides and decomposition route of Au(I) species **2a** and **2b**, and synthesis of **cis-7a-Cl** by oxidative addition of an aryl diazonium salt. NMR yield of the reactions calculated using 1,3,5-trimethoxybenzene as internal standard. (b) Crystal structures of **cis-7a-Cl**, **8a-OMe**, **9a** and **8b-OMe** (ellipsoids set at 50% probability, H atoms removed for clarity; for **cis-7a-Cl**, **BF4**⁻ anion is removed for clarity; for **8a-OMe** and **9a**, **SbF6**⁻ anion is not shown for clarity). Selected bond distances for **cis-7a-Cl** (Å): Au1–C10 2.009(7), Au1–N3 2.154(7), Au1–C38 2.006(8), Au1–Cl2 2.303(2).

salts with either alkenamines, alkenols or alkenoic acids, using $[(\text{Ph}_3\text{P})\text{AuCl}]$ under photo-free conditions.⁶⁹ Thus, we envisioned that our $\text{MIC}^{\text{N}}/\text{Au(I)}$ system should afford γ -benzyl- γ -butyrolactone products when reacting aryl iodides with γ -alenoic acids, *via* coupling/lactonization, provided the oxidative addition step takes place (see reaction scheme embedded in Table 1). Our first attempts consisted in a stoichiometric reaction between 4-iodoanisole, 4-pentenoic acid, complex **2b**, K_3PO_4 , and AgSbF_6 at 80 °C. When the reactions were carried out in the presence of an excess of base or AgSbF_6 , we did not observe any conversion, probably due to the rapid decomposition of the Au(I) complex. We also found that by using chlorinated solvents such as 1,2-dichloroethane, the conversion reached up to 49% (Table S3†). We determined by ¹H NMR analysis that the catalyst decomposes under the reaction conditions, forming the triazolium salt **1b**. Interestingly, the

conversion was significantly higher using 2,2,2-trifluoroethanol (TFE) (up to 92%) instead of 1,2-dichloroethane (Table 1 and S3†). When the reaction was carried out at 100 °C, the conversion was quantitative, but the yield was very similar to that found at 80 °C (67% yield at 100 °C vs. 63% yield at 80 °C, entries 1–2 in Table 1), and we also observed the formation of the triazolium salt **8b-OMe**. This was a strong indication that complex **2b** underwent an oxidative addition of the $\text{C}_{\text{sp}^2}\text{–I}$ bond, but rapid reductive elimination to form the coupling product **8b-OMe** occurred.

With these results in hand, we explored the possibility to perform the catalytic version of the arylation-lactonization of γ -alenoic acids. Thus, we carried out the reaction decreasing the loading of **2b**, first using substoichiometric 70 mol% of the gold complex. Product **10** was obtained in 65% yield (entry 3), so effectively a quantitative transformation was achieved with

Table 1 Synthesis of γ -benzyl- γ -butyrolactone 10 promoted by complex 2b^a

Entry	[Ag] (eq.)	[Au] mol%	K ₃ PO ₄ (eq.)	Solvent	Conversion% (yield%)
				2b	
1 ^b	2.8	100	1.0	TFE	92(63)
2 ^{b,c}	2.6	100	1.2	TFE	>99(67)
3 ^d	2.2	70	1.2	TFE	81(65)
4 ^d	2.0	40	1.1	TFE	79(44)
5 ^b	1.5	10	1.0	TFE	51(28)
6	1.5	10	0.5	TFE	51(24)
7 ^d	1.5	10	1.1	TFE	54(15)
8 ^d	1.1	1	0.5	TFE	38(1.6)
9	1.5	10	1.0	HFIP	56(29)

^a Reaction conditions: [Ar-I] = 0.08 M, [4-pentenoic acid] = 0.08 M, 80 °C, 16 h. V = 0.55 – 1.40 mL (¹H NMR yield obtained with 1,3,5-trimethoxybenzene as internal standard). ^b [Ar-I] = 0.02 M, [4-pentenoic acid] = 0.1 M, V = 1 mL. ^c T = 100 °C. ^d Reaction time = 24 h.

respect to Au loading. By using 40 mol% of Au(I) complex the yield was 44%, reaching about 1 TON (entry 4). Interestingly, using a lower amount of 2b (10 mol%) the yield was around 28% (~3 TON, entry 5). Similarly, by using hexafluoro-2-propanol (HFIP) the yield was 29% (~3 TON, entry 9); therefore, the best optimized results were obtained with fluorinated alcohols.

To exclude the possibility of oxidizing Au(I) to Au(III) in the presence of Ag(I), complex 2a (1 eq.) was reacted with AgSbF₆ (15 eq.) in HFIP at 80 °C for 16 hours. Quantitative formation of the Au(I) dimer 3a was observed by NMR, confirming the role of silver as halide scavenger (see Scheme S12†).

The scope of the reaction was examined with different aryl halides and γ -alkenoic acids (Fig. 5). The arylation-lactonization using iodobenzene and complex 2b reached 50% yield (~5 TON) in product 11. As expected, by increasing the catalyst loading to 20 mol%, the yield of 11 increased up to 87%, thus maintaining the turnover number (~4–5 TON). Gratifyingly, the best yields were reached using 4-iodotoluene, obtaining product 12 in 60% yield using 2a (~6 TON) and 81% yield using 2b (~8 TON). However, the presence of the strong electron-withdrawing group CF₃ in the *para*-position of the iodoaryl produced product 13 in a lower yield (~13%). Following this trend,^{36,38} 1-iodo-4-nitrobenzene produced a more dramatic drop of the yield of the corresponding product 14 (1%).

Interestingly, the γ -alkenoic acid with α -methyl groups reacted smoothly, yielding 37% of 15 using 2a and 41% of 15 using 2b. Also, complexes 2a and 2b performed very similar, except in the case of using iodobenzene and 4-pentenoic acid, yet complex 2b is almost two-fold more active than 2a (31% vs. 50% yield of compound 11, for 2a and 2b, respectively). The molecular structure of compound 16 was determined by X-ray diffraction analysis and revealed the formation of the (*R*)-enantiomer by spontaneous resolution.

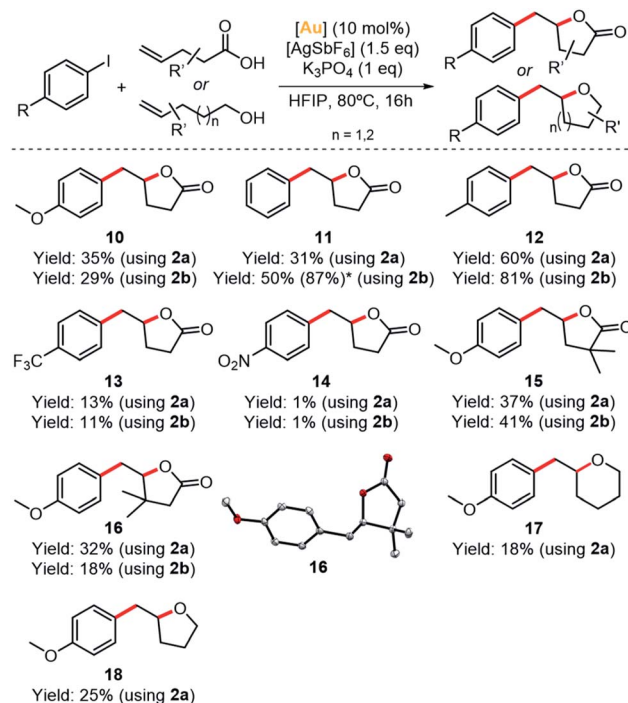


Fig. 5 Scope of the arylation-lactonization of alkenoic acids (10–16) and oxyarylation of alkenes (17–18). *NMR yield using 20% of [Au] is shown in parenthesis. Crystal structure of 16 is shown (ellipsoids set at 50% probability, H atoms removed for clarity).

Finally, in order to broaden the scope of these (MIC^N)Au(I) complexes, we tested complex 2a in the oxyarylation of alkenols and 1,2-diarylation of alkenes under the same catalytic conditions (Scheme S11†). The oxyarylation products 17 and 18 were obtained in low but significant yields (18–25%, ~2 TON) (Fig. 5 and Table S6†). On the contrary, the 1,2-diarylation reaction was unsuccessful.

Based on the fundamental understanding of the redox behaviour of complexes 2a and 2b, and the previously reported gold-catalyzed processes combining aryl halide oxidative addition and π -activation of alkenes,⁵³ a mechanistic proposal is depicted in Fig. 6. First, the oxidative addition of the C_{sp²}–I bond into a cationic gold(I) species occurs, affording a cationic aryl-gold(III) species. Then, the silver salt abstracts the iodide from this Au(III) species to generate a vacant site that can be occupied by the π -coordination of the olefin. Subsequent intramolecular γ -lactonization is enabled by the presence of base and the π -activation of the alkene produced by the gold center, to yield an alkylaryl gold(III) intermediate. The latter is proposed to undergo a reductive elimination step that affords the γ -benzyl- γ -butyrolactone product and closes the catalytic cycle by regenerating the initial catalytically active hemilabile [Au^I-(MIC^N)⁺ species].

To gain mechanistic insight, the stoichiometric reaction of *cis*-7a-Cl with AgSbF₆ (1.2 eq.), 4-pentenoic acid (1.3 eq.) and K₃PO₄ (1.0 eq.) was carried out in HFIP at 80 °C. After 16 hours, γ -benzyl- γ -butyrolactone 10 was obtained in 73% yield (Scheme S13†). Therefore, it is plausible to propose the formation of an



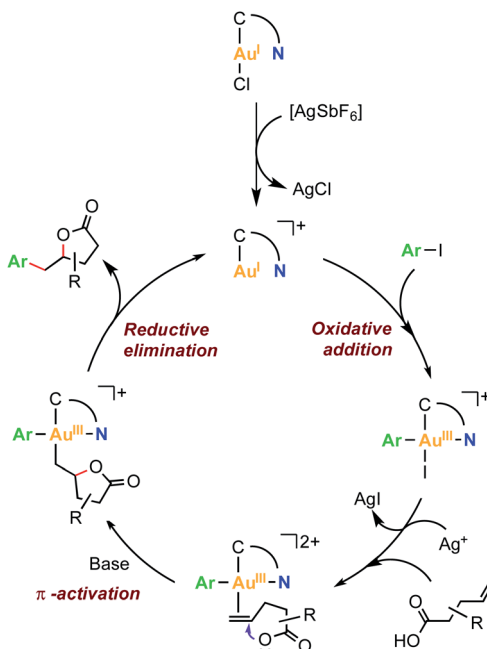


Fig. 6 Proposed reaction mechanism for the Au(I)/Au(III)-mediated arylation-lactonization of alkenoic acids.

arylgold(III) intermediate formed by an oxidative addition reaction of the C_{sp^2} -I bond to Au(I).

Conclusions

We synthesized two Au(I) complexes bearing bidentate hemilabile MIC^N ligands, $[Au^I(MIC^N)Cl]$, **2a** and **2b**, and explored their redox reactivity. The formation of the Au(III) complexes **4a-Cl** and **4a-OAc** was achieved by using $2 e^-$ oxidants of the type $PhIX_2$ ($X = Cl, OAc$), demonstrating a suitable design of the MIC^N ligand to stabilize Au(III) centers. Next, we showed that effective oxidative addition of a strained C_{sp^2} - C_{sp^2} bond was obtained when reacting **2b** with biphenylene in the presence of a halide scavenger and heating at $90^\circ C$. In this case, complex **5b** was obtained as the desired ensuing Au(III) species.

On the other hand, the oxidative addition of aryl iodides to Au(I) required a temperature of $120^\circ C$, and under these conditions the reductive elimination reaction of Au(III) species is also favored, yielding a series of triazolium salts (**8a-R**/**8b-R**, **9a**/**9b** and **1a**/**1b**). Although the expected Au(III) complexes were not directly detected, we independently synthesized the analogous Au(III) complex **cis-7a-Cl**, which after heating produced the same triazolium product (**8a-OMe**), thus supporting the oxidative addition/reductive elimination pathway for aryl iodides.

Finally, we combined all the redox knowledge gained with this system to develop a novel reaction for the synthesis of γ -benzyl- γ -butyrolactones upon arylation-lactonization of γ -alenoic acids. The reaction was catalyzed by **2a** and **2b** (10 mol% catalyst loading), obtaining up to 8 TON. The catalytic activity shown by MIC^N /Au system is significant because it shows that readily available hemilabile C^N ligands are a real alternative to

hemilabile P^N ligands, where MeDalphos system stands out among catalytic examples of oxidant-free oxidative addition of aryl halides allowed by the presence of pendant N-groups. Current efforts are devoted to extending the application of these hemilabile $[Au^I(MIC^N)Cl]$ complexes to novel catalytic transformations.

Data availability

Data for this work, including experimental procedures, NMR spectra and crystallographic data, are provided in the ESI.†

Author contributions

P. F., H. V. and G. G.-B. performed the experiments. All authors discussed the results and wrote the manuscript.

Conflicts of interest

There are no conflicts to declare.

Acknowledgements

We acknowledge financial support from MINECO of Spain for projects CTQ2016-77989-P, PID2019-104498GB-I00, RTI2018-098903-J-100 and PID2021-122900NB-I00 (financed by MICIN/AEI/10.13039/ 501100011033/ FEDER “Una manera de hacer Europa”), and for a FPU PhD grant to P. F. We also thank the Generalitat de Catalunya for project 2017SGR264 to X. R. and for a Beatriu de Pinós contract to H. V. (Beatriu de Pinós, 2019-BP-0080). X. R. is grateful for an ICREA Acadèmia award. G. G.-B gratefully acknowledges (RYC2019-026693-I/AEI/10.13039/ 501100011033) “El Fondo Social Europeo invierte en tu futuro”. Gobierno de Aragón/FEDER, UE (GA/FEDER, Reactividad y catálisis en química inorgánica, Group E50_20D). The authors would like to acknowledge the ‘Servicio General de Apoyo a la Investigación-SAI, Universidad de Zaragoza’, and the STR-UdG for technical support.

Notes and references

- 1 R. Dorel and A. M. Echavarren, *Chem. Rev.*, 2015, **115**, 9028–9072.
- 2 A. S. K. Hashmi, *Chem. Rev.*, 2007, **107**, 3180–3211.
- 3 A. Fürstner and P. W. Davies, *Angew. Chem., Int. Ed.*, 2007, **46**, 3410–3449.
- 4 J. H. Teles, S. Brode and M. Chabanas, *Angew. Chem., Int. Ed.*, 1998, **37**, 1415–1418.
- 5 Y. Fukuda and K. Utimoto, *J. Org. Chem.*, 1991, **56**, 3729–3731.
- 6 A. S. K. Hashmi, T. M. Frost and J. W. Bats, *J. Am. Chem. Soc.*, 2000, **122**, 11553–11554.
- 7 M. N. Hopkinson, A. D. Gee and V. Gouverneur, *Chem. – Eur. J.*, 2011, **17**, 8248–8262.
- 8 A. Nijamudheen and A. Datta, *Chem. – Eur. J.*, 2020, **26**, 1442–1487.



9 A. Kar, N. Mangu, H. M. Kaiser, M. Beller and M. K. Tse, *Chem. Commun.*, 2008, 386–388.

10 L. T. Ball, M. Green, G. C. Lloyd-Jones and C. A. Russell, *Org. Lett.*, 2010, **12**, 4724–4727.

11 L. T. Ball, G. C. Lloyd-Jones and C. A. Russell, *Chem. – Eur. J.*, 2012, **18**, 2931–2937.

12 G. Zhang, L. Cui, Y. Wang and L. Zhang, *J. Am. Chem. Soc.*, 2010, **132**, 1474–1475.

13 T. de Haro and C. Nevado, *J. Am. Chem. Soc.*, 2010, **132**, 1512–1513.

14 T. Ball Liam, C. Lloyd-Jones Guy and A. Russell Christopher, *Science*, 2012, **337**, 1644–1648.

15 L. T. Ball, G. C. Lloyd-Jones and C. A. Russell, *J. Am. Chem. Soc.*, 2014, **136**, 254–264.

16 X. C. Cambeiro, N. Ahlsten and I. Larrosa, *J. Am. Chem. Soc.*, 2015, **137**, 15636–15639.

17 M. Hofer, A. Genoux, R. Kumar and C. Nevado, *Angew. Chem., Int. Ed.*, 2017, **56**, 1021–1025.

18 M. Livendahl, P. Espinet and A. M. Echavarren, *Platinum Met. Rev.*, 2011, **55**, 212–214.

19 T. Lauterbach, M. Livendahl, A. Rosellón, P. Espinet and A. M. Echavarren, *Org. Lett.*, 2010, **12**, 3006–3009.

20 M. Livendahl, C. Goehry, F. Maseras and A. M. Echavarren, *Chem. Commun.*, 2014, **50**, 1533–1536.

21 D. J. Gorin and F. D. Toste, *Nature*, 2007, **446**, 395–403.

22 M. Joost, A. Amgoune and D. Bourissou, *Angew. Chem., Int. Ed.*, 2015, **54**, 15022–15045.

23 B. Huang, M. Hu and F. D. Toste, *Trends Chem.*, 2020, **2**, 707–720.

24 P. Font and X. Ribas, *Eur. J. Inorg. Chem.*, 2021, **2021**, 2556–2569.

25 M. N. Hopkinson, A. Tlahuext-Aca and F. Glorius, *Acc. Chem. Res.*, 2016, **49**, 2261–2272.

26 S. Banerjee, V. W. Bhoyare and N. T. Patil, *Chem. Commun.*, 2020, **56**, 2677–2690.

27 M. O. Akram, S. Banerjee, S. S. Saswade, V. Bedi and N. T. Patil, *Chem. Commun.*, 2018, **54**, 11069–11083.

28 J. Miró and C. del Pozo, *Chem. Rev.*, 2016, **116**, 11924–11966.

29 V. W. Bhoyare, A. G. Tathe, A. Das, C. C. Chintawar and N. T. Patil, *Chem. Soc. Rev.*, 2021, **50**, 10422–10450.

30 N. Lassauque, P. Gualco, S. Mallet-Ladeira, K. Miqueu, A. Amgoune and D. Bourissou, *J. Am. Chem. Soc.*, 2013, **135**, 13827–13834.

31 P. Gualco, S. Ladeira, K. Miqueu, A. Amgoune and D. Bourissou, *Angew. Chem., Int. Ed.*, 2011, **50**, 8320–8324.

32 J. Guenther, S. Mallet-Ladeira, L. Estevez, K. Miqueu, A. Amgoune and D. Bourissou, *J. Am. Chem. Soc.*, 2014, **136**, 1778–1781.

33 J. Serra, T. Parella and X. Ribas, *Chem. Sci.*, 2017, **8**, 946–952.

34 H. Beucher, J. Schörgenhummer, E. Merino and C. Nevado, *Chem. Sci.*, 2021, **12**, 15084–15089.

35 C.-Y. Wu, T. Horibe, C. B. Jacobsen and F. D. Toste, *Nature*, 2015, **517**, 449–454.

36 M. Joost, A. Zeineddine, L. Estévez, S. Mallet-Ladeira, K. Miqueu, A. Amgoune and D. Bourissou, *J. Am. Chem. Soc.*, 2014, **136**, 14654–14657.

37 M. Joost, L. Estévez, K. Miqueu, A. Amgoune and D. Bourissou, *Angew. Chem., Int. Ed.*, 2015, **54**, 5236–5240.

38 M. J. Harper, C. J. Arthur, J. Crosby, E. J. Emmett, R. L. Falconer, A. J. Fensham-Smith, P. J. Gates, T. Leman, J. E. McGrady, J. F. Bower and C. A. Russell, *J. Am. Chem. Soc.*, 2018, **140**, 4440–4445.

39 J. A. Cadge, H. A. Sparkes, J. F. Bower and C. A. Russell, *Angew. Chem., Int. Ed.*, 2020, **59**, 6617–6621.

40 J. Chu, D. Munz, R. Jazza, M. Melaimi and G. Bertrand, *J. Am. Chem. Soc.*, 2016, **138**, 7884–7887.

41 A. Zeineddine, L. Estévez, S. Mallet-Ladeira, K. Miqueu, A. Amgoune and D. Bourissou, *Nat. Commun.*, 2017, **8**, 565.

42 J. Rodriguez, A. Tabey, S. Mallet-Ladeira and D. Bourissou, *Chem. Sci.*, 2021, **12**, 7706–7712.

43 D. Mendoza-Espinosa, D. Rendon-Navar, A. Alvarez-Hernandez, D. Angeles-Beltran, G. E. Negron-Silva and O. R. Suarez-Castillo, *Chem.-Asian J.*, 2017, **12**, 203–207.

44 G. Kleinhans, M. M. Hansmann, G. Guisado-Barrios, D. C. Liles, G. Bertrand and D. I. Bezuidenhout, *J. Am. Chem. Soc.*, 2016, **138**, 15873–15876.

45 G. Kleinhans, A. K. Chan, M. Y. Leung, D. C. Liles, M. A. Fernandes, V. W. Yam, I. Fernandez and D. I. Bezuidenhout, *Chem. – Eur. J.*, 2020, **26**, 6993–6998.

46 R. P. Herrera and M. C. Gimeno, *Chem. Rev.*, 2021, **121**, 8311–8363.

47 L. Huang, F. Rominger, M. Rudolph and A. S. K. Hashmi, *Chem. Commun.*, 2016, **52**, 6435–6438.

48 A. Tabey, M. Berlande, P. Hermange and E. Fouquet, *Chem. Commun.*, 2018, **54**, 12867–12870.

49 J. Rodriguez, A. Zeineddine, E. D. Sosa Carrizo, K. Miqueu, N. Saffon-Merceron, A. Amgoune and D. Bourissou, *Chem. Sci.*, 2019, **10**, 7183–7192.

50 J. Rodriguez, D. Vesseur, A. Tabey, S. Mallet-Ladeira, K. Miqueu and D. Bourissou, *ACS Catal.*, 2022, **12**, 993–1003.

51 M. O. Akram, A. Das, I. Chakrabarty and N. T. Patil, *Org. Lett.*, 2019, **21**, 8101–8105.

52 J. Rodriguez, N. Adet, N. Saffon-Merceron and D. Bourissou, *Chem. Commun.*, 2020, **56**, 94–97.

53 M. Rigoulet, O. Thillaye du Boullay, A. Amgoune and D. Bourissou, *Angew. Chem., Int. Ed.*, 2020, **59**, 16625–16630.

54 A. G. Tathe, C. C. Chintawar, V. W. Bhoyare and N. T. Patil, *Chem. Commun.*, 2020, **56**, 9304–9307.

55 S. Zhang, C. Wang, X. Ye and X. Shi, *Angew. Chem., Int. Ed.*, 2020, **59**, 20470–20474.

56 A. G. Tathe, Urvashi, A. K. Yadav, C. C. Chintawar and N. T. Patil, *ACS Catal.*, 2021, **11**, 4576–4582.

57 C. C. Chintawar, A. K. Yadav and N. T. Patil, *Angew. Chem., Int. Ed.*, 2020, **59**, 11808–11813.

58 S. R. Mudshinge, Y. Yang, B. Xu, G. B. Hammond and Z. Lu, *Angew. Chem., Int. Ed.*, 2022, **61**, e202115687.

59 X. Ye, C. Wang, S. Zhang, Q. Tang, L. Wojtas, M. Li and X. Shi, *Chem. – Eur. J.*, 2022, e202201018.

60 C. C. Chintawar, V. W. Bhoyare, M. V. Mane and N. T. Patil, *J. Am. Chem. Soc.*, 2022, **144**, 7089–7095.

61 T. Shibata, R. Nagai, S. Okazaki, S. Nishibe and M. Ito, *Bull. Chem. Soc. Jpn.*, 2022, **95**, 700–706.



62 E. Tomás-Mendivil, P. Y. Toullec, J. Borge, S. Conejero, V. Michelet and V. Cadierno, *ACS Catal.*, 2013, **3**, 3086–3098.

63 A. G. Nair, R. T. McBurney, M. R. D. Gatus, S. C. Binding and B. A. Messerle, *Inorg. Chem.*, 2017, **56**, 12067–12075.

64 M. Navarro, A. Tabey, G. Szalóki, S. Mallet-Ladeira and D. Bourissou, *Organometallics*, 2021, **40**, 1571–1576.

65 G. Guisado-Barrios, M. Soleilhavoup and G. Bertrand, *Acc. Chem. Res.*, 2018, **51**, 3236–3244.

66 J. Lorkowski, P. Źak, M. Kubicki, C. Pietraszuk, D. Jędrziewicz and J. Ejfler, *New J. Chem.*, 2018, **42**, 10134–10141.

67 K. J. Cavell and A. T. Normand, in *N-Heterocyclic Carbenes in Transition Metal Catalysis and Organocatalysis*, ed. C. S. J. Cazin, Springer, Dordrecht, 2010, vol. 32, pp. 299–314.

68 C. M. Crudden and D. P. Allen, *Coord. Chem. Rev.*, 2004, **248**, 2247–2273.

69 B. Dong, H. Peng, S. E. Motika and X. Shi, *Chem. – Eur. J.*, 2017, **23**, 11093–11099.

